Since January 2020 Elsevier has created a COVID-19 resource centre with free information in English and Mandarin on the novel coronavirus COVID-19. The COVID-19 resource centre is hosted on Elsevier Connect, the company's public news and information website.

Science of the Total Environment 753 (2021) 142238

Contents lists available at ScienceDirect

Science of the Total Environment

journal homepage: www.elsevier.com/locate/scitotenv

Substantial nitrogen oxides emission reduction from China due to COVID-19 and its impact on surface ozone and aerosol pollution

Qianqian Zhang [a], Yuepeng Pan [b,*], Yuexin He [b], Wendell W. Walters [c,d], Qianyin Ni [e], Xuyan Liu [a], Guangyi Xu [f], Jiali Shao [a], Chunlai Jiang [g]

[a] National Satellite Meteorological Center, China Meteorological Administration, Beijing 100081, China
[b] State Key Laboratory of Atmospheric Boundary Layer Physics and Atmospheric Chemistry, Institute of Atmospheric Physics, Chinese Academy of Sciences, Beijing 100029, China
[c] Department of Earth, Environmental, and Planetary Sciences, Brown University, Providence, RI 02912, USA
[d] Institute at Brown for Environment and Society, Brown University, Providence, RI 02912, USA
[e] Sinopec Yanshan Petrochemical Company, Beijing 102500, China
[f] Hebei Provincial Academy of Environmental Sciences, Shijiazhuang 050037, China
[g] Research Center for Total Pollution Load Control and Emission Trading, CAEP, Beijing 100012, China

HIGHLIGHTS

- NO_x emission in the lockdown period is 53.4% lower than the same period in 2019.
- East China experienced greater influence from COVID-19 than national mean level.
- NO_x decline leads to 36.5% O_3 increase and 12.5% $PM_{2.5}$ decrease over East China.
- Elevated O_3 enhances secondary aerosols formation through heterogeneous pathway.

GRAPHICAL ABSTRACT

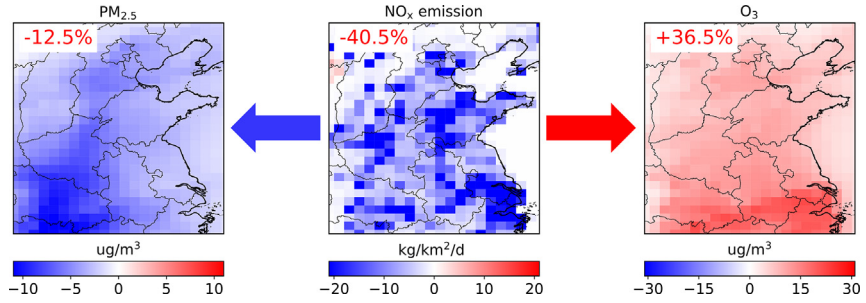

ARTICLE INFO

Article history:
Received 21 June 2020
Received in revised form 3 September 2020
Accepted 4 September 2020
Available online 6 September 2020

Editor: Pingqing Fu

Keywords:
NO_x emissions
Covid-19
Aerosols
Ozone
Control strategy

ABSTRACT

A top-down approach was employed to estimate the influence of lockdown measures implemented during the COVID-19 pandemic on NO_x emissions and subsequent influence on surface $PM_{2.5}$ and ozone in China. The nation-wide NO_x emission reduction of 53.4% due to the lockdown in 2020 quarter one in China may represent the current upper limit of China's NO_x emission control. During the Chinese New Year Holiday (P2), NO_x emission intensity in China declined by 44.7% compared to the preceding 3 weeks (P1). NO_x emission intensity increased by 20.3% during the 4 weeks after P2 (P3), despite the unchanged NO_2 column. It recovered to 2019 level at the end of March (P4). The East China (22°N - 42°N, 102°E - 122°E) received greater influence from COVID-19. Overall NO_x emission from East China for 2020 first quarter is 40.5% lower than 2019, and in P4 it is still 22.9% below the same period in 2019. The 40.5% decrease of NO_x emission in 2020 first quarter in East China lead to 36.5% increase of surface O_3 and 12.5% decrease of surface $PM_{2.5}$. The elevated O_3 promotes the secondary aerosol formation through heterogeneous pathways. We recommend that the complicated interaction between $PM_{2.5}$ and O_3 should be considered in the emission control strategy making process in the future.

1. Introduction

Beginning in December of 2019, the COVID-19 pandemic was first reported in Wuhan and rapidly evolved across the globe. China took

* Corresponding author.
E-mail address: panyuepeng@mail.iap.ac.cn (Y. Pan).

https://doi.org/10.1016/j.scitotenv.2020.142238
0048-9697/

decisive action to combat the spread of COVID-19 that included the lockdown of Wuhan as of Jan 23, 2020, stay-at-home orders during the Chinese New Year Holiday (Jan 24–Feb 2, 2020), and the shutdown of non-essential businesses. People gradually went back to work commencing on Feb 3, and energy demands, factory production, and vehicular traffic gradually recovered (Myllyvirta, 2020).

Nitrogen oxides ($NO_x = NO + NO_2$), a key component of the atmosphere, are mainly emitted from fossil-fuel combustion activities (Bauwens et al., 2020; Zhao et al., 2013). Thus, NO_x emissions are closely linked to human activities and respond quickly to economic changes. A dramatic decrease in nitrogen dioxide (NO_2) columns over China from satellite measurements were observed during February of 2020 (Bauwens et al., 2020; Liu et al., 2020), and NO_x emissions are expected to decrease accordingly (Ding et al., 2020; Zhang et al., 2020). Zhang et al. (2020) has calculated NO_x emission changes from East China from Jan 1 to Mar 12, 2020, and Ding et al. (2020) estimated NO_x emission from Chinese cities due to the COVID-19 lockdown. They focus on NO_x emission changes from regional or individual cites, but did not evaluate NO_x emissions from the whole China and regional difference for each period before, during and after the lockdown period in 2020. In addition, comparison of 2020 NO_x emision with those in -past years is also lacked to thoroughly understand changes in NO_x emissions associated with COVID-19.

NO_x play a crutial role in atmospheric chemistry, being precursors of both fine particle ($PM_{2.5}$) and ozone (O_3). NO_x are oxidized by hydroxyl (OH) and O_3 in the atmosphere to form nitric acid (HNO_3) and then nitrate, which is an important component of $PM_{2.5}$ (Wang et al., 2013). NO_x undergoes a series of photochemical reaction to generate O_3. During the lockdown period in 2020, emission reduction of primary air pollutants, including NO_x result in remarkable decrease in surface observed $PM_{2.5}$ concentration (Shi and Brasseur, 2020). On the other hand, increase in O_3 and radicals due to NO_x emission reduction leads to secondary aerosol formation and haze events during the lockdown period in 2020 (Huang et al., 2020; Le et al., 2020). However, there is no quantification of $PM_{2.5}$ and O_3 sensitivity to NOx emission change during COVID-19 in published works. To what extent the NO_x emission reduction in 2020 quarte one can impact surface air quality is still unclear.

In this study, we aim to evaluate the influence of NO_x emission changes for 2020 quarter one on both $PM_{2.5}$ and O_3 pollution over China. First we use a top-down method to assess NO_x emissions from China for the periods before, during, and after the Chinese New Year Holiday, and we also provide a historical context by a comparison with NO_x emission in 2019. Then we estimate $PM_{2.5}$ and O_3 changes due to NO_x emission change through a model study.

2. Methodology

2.1. TROPOMI NO_2 retrieval

The TROPOMI onboard the S—5P mission provides tropospheric NO_2 with a spatial resolution of up to 3.5×5.5 km^2. Tropospheric NO_2 vertical column density (VCD) was retrieved through a three-step procedure using the DOMINO approach (Boersma et al., 2011; van Geffen et al., 2020). First, the slant column density (SCD) is obtained by a differential optical absorption spectroscopy (DOAS) technique. Second, the stratospheric component of SCD is separated via data assimilation using a chemical transport model (CTM/DA). Finally, tropospheric VCD is acquired by dividing SCD by the tropospheric air mass factor (AMF) computed by the TM5 CTM.

Tropospheric NO_2 VCD is sensitive to the NO_2 vertical profile shape used in calculating AMF (Lamsal et al., 2010). The tropospheric AMF was calculated based on GEOS-Chem simulation and used in replacement of the a priori TM5 NO_2 profiles to diminish inconsistencies between model and satellite NO_2 columns (Boersma et al., 2016; Lamsal et al., 2010; Visser et al., 2019). Tropospheric NO_2 VCDs obtained using AMF calculated from TM5, and GEOS-Chem NO_2 profiles are referred to as TROPOMI^{TM5} and TROPOMI^{GC}, respectively. The difference between the two sets of tropospheric NO_2 VCD is shown in Fig. S1. Overall, the two sets of data correlate well with each other, with the correlation coefficient $r \geq 0.90$. The discrepancy between TROPOMI^{GC} and TROPOMI^{TM5} is small over China (bias within $\pm 5\%$). TROPOMI^{GC} is <20% higher than TROPOMI^{TM5} over South Korea and India. The disagreement between the two datasets can be attributed to the employment of different emission inventories within these models (Vinken et al., 2014).

For quality assurance, we use the TROPOMI data with a qa_value above 0.5, and only pixels with valid data for more than 3 days in each week were selected.

2.2. GEOS-Chem model and bottom-up inventory

In this study, we employ version v11–1 of the model to conduct a series of simulations to probe changes in NO_x emissions. The nested grid version of the GEOS-Chem model has a horizontal resolution of 0.5°-(latitude) × 0.625°(longitude) over East Asia (60°E - 150°E, 10°S - 55°N), and is driven by the MERRA-2 reanalysis meteorological field. We used the global simulation with 2°(latitude) × 2.5°(longitude) grids to provide the boundary condition (Zhang et al., 2018, 2019) All simulations were run from December 2018 to March 2019 and December 2019 to March 2020. In these simulations, the first month was used for spin-up and the subsequent three months for analysis.

Global anthropogenic NO_x emissions were taken from EDGAR v4.2 (EC-JRC/PBL, http://edgar.jrc.ec.europa.eu) and overwritten by MIX inventory (Li et al., 2017) over East Asia. Natural NO_x emissions include biomass burning sources from GFED v4.1, soil sources from Hudman et al. (2012), and lightning described by Murray et al. (2012). The default anthropogenic NO_x and relevant $PM_{2.5}$ and O_3 precursors in MIX inventory are scaled from 2010 to 2019 following Xu et al. (2020) (Fig. S2).

2.3. Top-down NO_x emission estimation

We use the mass balance procedure developed by Martin (2003) and Lamsal et al. (2011) and improved by Vinken et al. (2014) and Visser et al. (2019) to estimate the top-down NO_x emissions using TROPOMI/NO_2 column and GEOS-Chem model. This method takes into account the fact that NO_2 VCD responds non-linearly to surface NO_x emission change. We perform a sensitivity study by perturbing surface NO_x emission by 15% to get the scaling factor β, which denotes relative change of simulated NO_2 VCD due to a 1% change in NO_x emission. The influence of NO_x emission on the tropospheric AMF calculation (the dimensionless factor γ) is also considered following Visser et al. (2019). The equation used to estimate top-down NO_x emission (E_{td}) based on bottom-up NO_x emission (E_{bu}), TROPOMI NO_2 VCD with AMF from GEOS-Chem using bottom-up NO_x emission ($C_{TROPOMI^{GC,\,bu}}$) and simulated NO_2 VCD using bottom-up NO_x emission ($C_{GC,\,bu}$) is as follows:

$$E_{td} = E_{bu}\left(1 + \beta(1+\gamma)\frac{C_{TROPOMI^{GC,bu}} - C_{GC,bu}}{C_{GC,bu}}\right).$$

The scale factor β and γ are calculated using the following equations:

$$\beta = \frac{0.15}{\left(C_{GC,1.15bu} - C_{GC,bu}\right)/C_{GC,bu}}$$

$$\gamma = \frac{\left(C_{TROPOMI^{GC},1.15bu} - C_{TROPOMI^{GC},bu}\right)/C_{TROPOMI^{GC},bu}}{\left(C_{GC,1.15bu} - C_{GC,bu}\right)/C_{GC,bu}}$$

Uncertainties exist in the top-down inventory estimation. First is the uncertainty of satellite data, which is mainly driven by the calculation of air mass factors, and it can amount to ±30% (Lorente et al., 2019). The second is the model performance in simulating atmospheric NO_x lifetime. GEOS-Chem simulates noontime hydroxyl (OH) concentration at Beijing for 2020 January to March mean of 1.5×10^6 molec/cm^3, which is lower than Tan et al. (2018) meatured for 2016 January and

February (2.4–3.6 × 10^6 molec/cm^3). The underestimation of OH concentration may lead to overestimation of NO_x lifetime, but it is difficult to quantify this uncertainty for lack of enough surface observation. Third, the Sentinel-5 Precursor (S—5P) mission has an equator crossing time near 13:30 local solar time. NO_x emissions derived from noontime NO_2 column may introduce uncertainty considering the diurnal variation of NO_x emissions. Fourth, the longer lifetime of NO_x during winter may result in transport of NO_2 from source regions ("smearing") and thus lead to bias of top-down emission estimation. We will validate our top-down NO_x emission inventory using surface NO_2 measurements and through comparison with NO_x emissions from other studies.

3. Results and discussion

3.1. NO_x emission

We conduct simulations for 2019 and 2020 first quarter with the top-down NO_x emission inventories for the two years, respectively. Simulated surface NO_2 concentration is compared with observations (Fig. S3). The model and observation correlates well with each other with an correlation coefficient of 0.64 for the two years, but the model tends to underestimate NO_2 concentration by more than 50%. Surface NO_2 measurements are monitored by the chemilumine scenceanalyzer which may lead to overestimate of NO_2 by about 50% due to interferences from other nitrogen species (Kharol et al., 2015; Zhang et al., 2016). If we simply cut the observed NO_2 concentration by 50%, model underestimation will decline to 4.5% for 2019 and 13.5% for 2020.

We divide the first quarter of 2019 and 2020 into four periods. The first period (P1) is 3-weeks before Chinese New Year holiday, the second period (P2) is the Chinese New Year holiday (2019 Feb 4–10 and 2020 Jan 23–Feb 2), and the third and fourth periods (P3 and P4) are 1–4- and 5–8-weeks after Chinese New Year holiday. Mean satellite retrieved NO_2 VCD are compared over the four periods for the year 2019 and 2020, and NO_x emissions were calculated at a weekly level.

3.1.1. Significant NO_x emission reduction in China from P1 to P2 and P3 period

Fig. 1 presents NO_x emission intensity (Gg/d) for each week before, during, and after the Chinese New Year Holiday. NO_x emissions for the whole China and the east part of China (EC, 112°E—122°E, 30°N—42°N) are given. The EC region has the largest population and the most serious air pollution in China. In Fig. 2 we display the mean NO_x emission intensity during the four periods of quarter one in 2020 and 2019, and the difference between the two years.

Overall, in 2020, NO_x emissions dropped steadily during P1. In P2, NO_x emission intensity from China was 44.7% lower than P1, slightly lower than NO_2 column change (Fig. 3, 49.0%). In contrast, the decrease in NO_x emission intensity in 2019 due to the New Year Holiday effect was only 20.9%. This indicates a much greater influence of the lockdown measures than the 'holiday effect' (Tan et al., 2009) on the reduction of NO_x emissions. We should also see that NO_x emission from EC experienced a greater influence from COVID-19. In 2020, the decrease rate from P1 to P2 was 52.1% in EC, and it was only 17.2% in 2019. Moreover, NO_x emission from EC makes up ~50% of the total NO_x emission from China in 2020 P1, 2019 P1 and P2, but it was only 41.2% in 2020 P2.

No increase in NO_x emission intensity was observed for the first week after the New Year Holiday, which was extended to combat the spread of COVID-19. Starting on Feb 10, 2020, more and more people went back to work, and NO_x emissions from China increased at an average 10.0% rate during the next two weeks. As of Mar 1, 2020, the fourth week after the Chinese New Year Holiday, NO_x emission from China was 43.0 Gg/d, which was 19.0% higher than the previous week and 47.0% higher than the New Year Holiday period. As a result, NO_x emission intensity from China increased by 20.3% from the 2020 New Year Holiday to the subsequent 4-week period despite the unchanged NO_2 columns, but was still 33.5% below the level of P1. By contrast, NO_x emission from

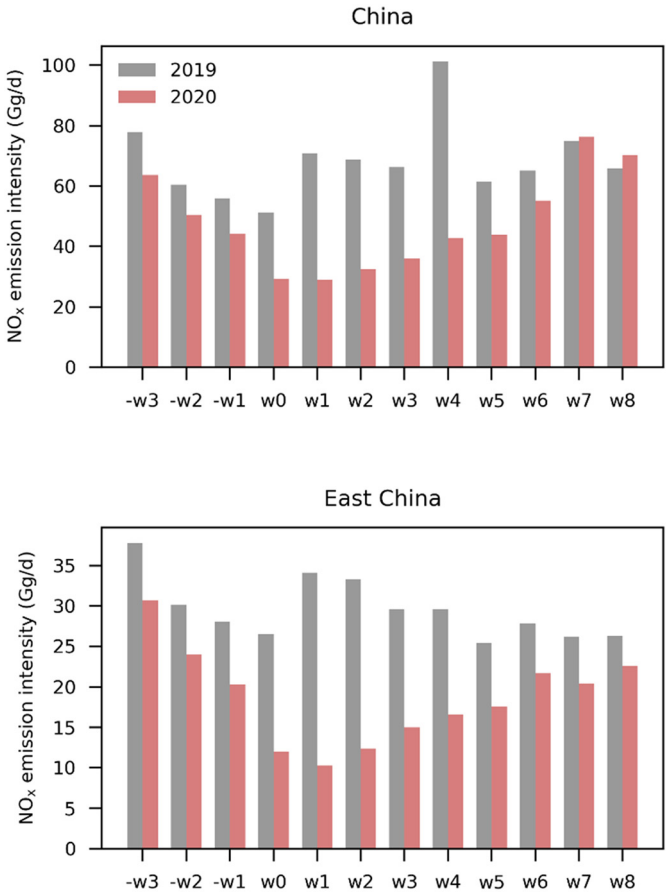

Fig. 1. Weekly NO_x emission intensity (Gg/d) in China (top) and East China (bottom) from 3 weeks before (−w3 ~ −w1) to 8 weeks after (w1 ~ w8) the Chinese New Year Holiday (w0).

EC in P3 only increased by 9.5% than P2, and was 42.3% lower than P1. The mean NO_x emission intensity from China for P2 and P3 (33.3 Gg/d) was 36.7% lower than P1. This difference was smaller than observed for NO_2 columns during the same periods of 49.8% (Fig. 3). The discrepancy between NO_x emission and NO_2 column differences can be explained by the shorter lifetime of NO_2 in February than in January.

Before the Chinese New Year Holiday, NO_x emissions from China was about 20% lower in 2020 than in 2019 (Fig. 2). This change in NO_x emissions reflects the long-term trend of decreasing NO_x emissions in China (Bauwens et al., 2020; Field et al., 2020), which has been an important and effective control strategy to combat air pollution. Following the holiday, differences in NO_x emission from China between 2020 and 2019 were greater than 40% and as high as 54.3% during P2 and P3 periods. This large discrepancy indicates a substantial reduction in NO_x emissions due to measures to combat COVID-19.

Our estimation of NO_x emission reductions due to lockdown is within reasonable bounds comparing to published works. Huang et al. (2020) reported a 60–70% reduction of NO_x emission from China due to the lockdown. Ding et al. (2020) estimated that NO_x emission from cities in East China have declined by 20–50%. Zhang et al. (2020) calculated that NO_x (22°N - 42°N, 102°E - 122°E) emissions from East China before and during the lockdown are 1589 and 795 Gg/month, respectively. Comparable to Zhang et al. (2020), our estimation of NO_x emissions from this region amount to 1348 Gg/month for P1 and 728 Gg/month for P2, respectively.

This is not the first time that a large decrease in air pollutant emissions has been observed over a short period. Previously, China implemented stringent regulations to reduce air pollutant emissions for some key events, such as the 2008 Olympic Games, 2014 Asia-Pacific

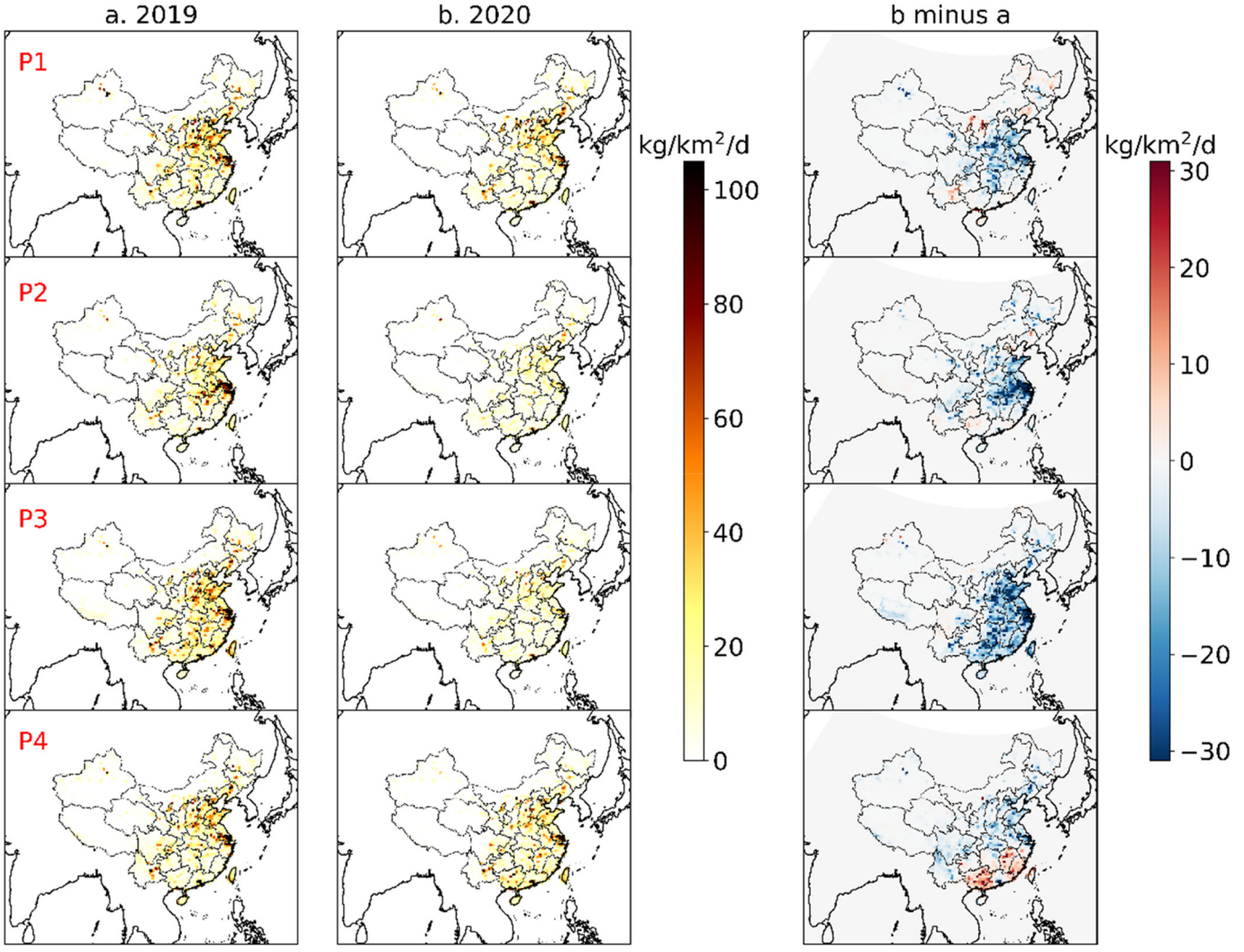

Fig. 2. NO_x emission intensity ($kg/km^2/d$) during the four periods in 2019 and 2020, and the difference between the two years. The size of each grid cell is 0.5°latitude × 0.625°longitude.

Economic Cooperation (APEC) Summit, and 2015 V-Day Military Parade. Indeed, Wang et al. (2010) reported a 47% decrease in NO_x emission from Beijing during the 2008 Olympic Games. Zhang et al. (2016) estimated a NO_x emission reduction of 33% in Beijing and 35% in Hebei province during the APEC period. However, these measurements are limited to Beijing and surrounding areas, and for a relatively short time. The pandemic of COVID-19 led to a nation-wide NO_x emission intensity reduction of 36.7% during the lockdown period (P2 and P3) compared to the pre-crisis (P1) level, and 53.4% compared to the same period in 2019. This may be the upper limit of NO_x emission control for China at the present level of economy and technology. Anthropogenic NO_x originates mainly from industry, power plants, and transportation sources. During the lockdown period, most of the business and industries were closed, and people stayed at home to avoid infection. Myllyvirta (2020) reported that coal use in power plants in China fell to a four-year low during the P2 and P3 periods. Crude oil processing of Sinopec dropped by more than 30% in February below the usual

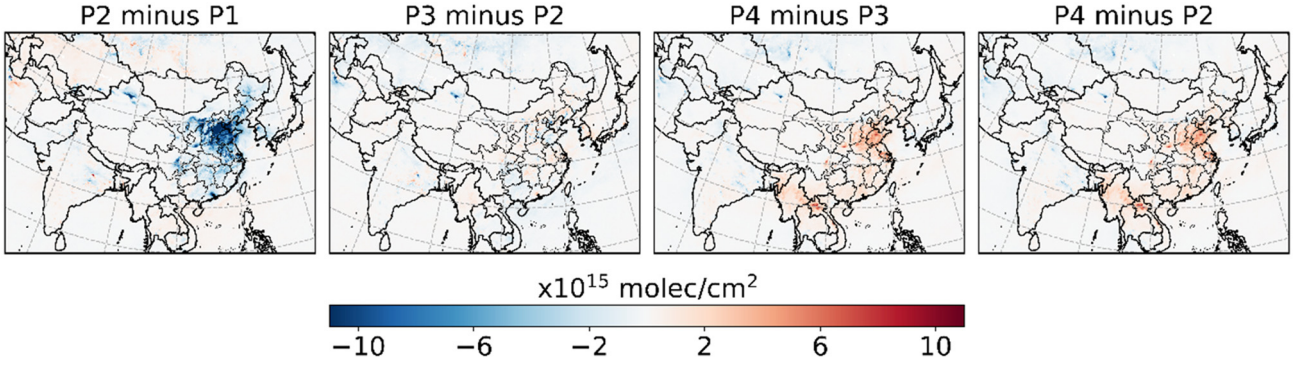

Fig. 3. The difference in NO_2 columns during the four periods of 2020 first quarter. The data is resampled at 0.1° × 0.1° grids.

level, and gasoline sales in Beijing during P2 and P3 were only a quarter of the normal level.

3.1.2. The rebound of NO_x emission in China during P4 period

As the economy rebounded and energy consumption increased, NO_x emission from China began to grow in March 2020. NO_x emission intensity during the sixth week (55.0 Gg/d) caught up with that during P1 (52.7 Gg/d). By Mar 29, NO_x emission intensity reached 70.4 Gg/d. Despite the relatively small change of NO_2 columns (32.5%), the average NO_x emission intensity from China in the P4 period was 75.1% higher than that in the P3 period, and more than twice that in the Chinese New Year Holiday. NO_x emission intensity during the P4 period in 2020 was only 8.2% less than in 2019. Furthermore, since the seventh week after Feb 3, China's NO_x emission intensity exceeds that in the same period in 2019, indicating a full rebound of NO_x emission from China at the end of the first quarter of 2020. However, NO_x emission from EC increased at a much slower rate than the national mean level in P4, and it was 22.9% lower than 2019 P4.

Myllyvirta (2020) reported that coal consumption in China returned to the normal range at about seven weeks after the New Year Holiday, and Sinopec crude oil processing during March went back to the normal level. On the other hand, gasoline sales in Beijing only recovered to 50% of the usual level by the end of March, which, to some extent, indicates that NO_x emission in EC will see a further increase as the recovery of gasoline sales in April and May.

In summary, the large decrease in NO_x emission during the lockdown period may be the upper limit of current NO_x emission control in China, and the COVID-19 has greater impact on NO_x emission from the EC region than the national mean. Rebound of NO_x emission from EC during P4 is weaker compared to the national mean.

3.2. influence of NO_x emission changes on surface O_3 and $PM_{2.5}$

After we calculate NO_x emissions from China in 2019 and 2020 first quarter, we use the two sets of emissions to evaluate impact of NO_x emission Change on $PM_{2.5}$ and O_3. To do so, we use the meteorology field for 2020 quarter one, emissions of all species but NO_x are scaled up to the year 2019 on the basis of 2010 MIX emission inventory (Fig. S2). We perform two simulations. In the first simulation we use top-down estimated NO_x emission for 2019 and in the second one we use that for 2020. The difference between the two simulations can be treated as influence of NO_x emission change. To distinguish the two simulations, we call the simulation with 2019 NO_x emission the standard simulation (STD), and the one with 2020 NO_x emission the optimized simulation (OPT). We have shown in Table S1 that the model can well capture the spatial distribution of observed O_3 and $PM_{2.5}$ over East China (correlation coefficient greater than 0.60) with acceptable bias (normalized mean bias within $\pm$30%).

Fig. 4 displays simulated 2020 first quarter mean O_3 and $PM_{2.5}$ distribution with 2019 and 2020 NO_x emissions, respectively, and the difference between the two years. Overall, 40.5% decrease in NO_x emission over EC leads to 36.5% increase in surface O_3 concentration. This indicates an overall NO_x-saturated (VOCs-limited) regime of ozone formation over EC during 2020 quarter one. Under this condition (NO_x-saturated), react with NO_2 to generate HNO_3 is the main sink of OH (Shah et al., 2020), and decrase of NO_x leaves more OH to form O_3. $PM_{2.5}$ responds positively with respect to NO_x emission change, 40.5% decrease of NO_x emission results in 12.5% decrease in $PM_{2.5}$ concentration over EC. We use the sensitivity factor η as introduced by (Zhang et al., 2015) to represent influence of NO_x emission change on $PM_{2.5}$ concentration. η value for each period is depicted in Table S2. η value increases as NO_x emission reduction rate incrases, because that as NO_x emission decreases, nitrate formation becomes more sensitive to NO_x emission change (Zhang et al., 2019).

Besides O_3, concentrations of some other atmospheric oxidants, such as HO_2, NO_3 radical and OH have also increased (Fig. S4). Increase of oxidants in the atmosphere will promote formation of secondary aerosols (Huang et al., 2020; Sun et al., 2020). Secondary aerosols form through homogeneous and heterogeneous pathways, and we find that the elevated oxidants may be more favorable for the heterogeneous pathway. We performed a sensitivity study in which the heterogeneous formation of nitrate is isolated. The result shows that, in the STD simulation,

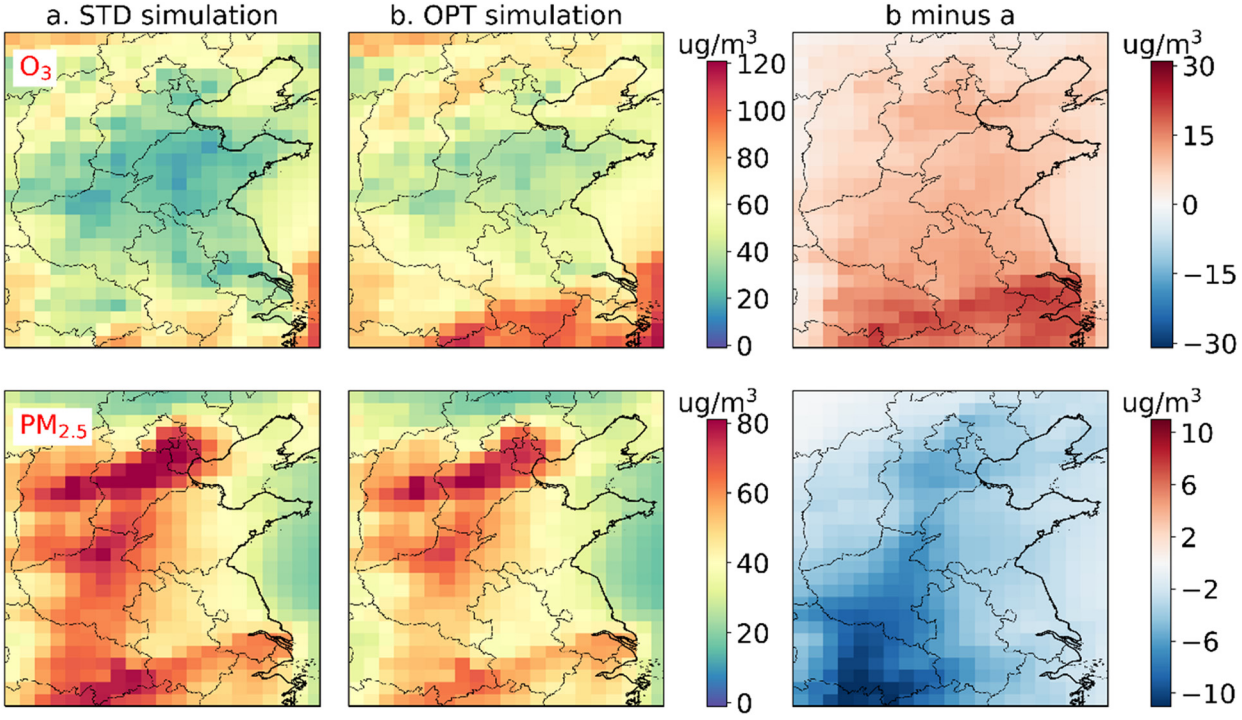

Fig. 4. simulated 2020 first quarter mean surface O_3 (top) and $PM_{2.5}$ (bottom) concentrations in STD simulation (left) and OPT simulation (middle), and the difference between them (right).

23.9% of nitrate is formed through uptake of N_2O_5 on aerosols, and in the OPT simulation, the fraction increases to 28.8%.

The large magnitude of decrease in NO_x emission during the lockdown period helps to abate the winter time haze pollution over Central North China. However, the elevated O_3 and relevant atmospheric oxidants' concentration favors the formation of secondary aerosol, especially through the heterogeneous pathway.

4. Conclusion

The outbreak of COVID-19 lead to substantial decrease of NO_x emission and air quality changes in China. The purpose of this study is to quantify the NO_x emission changes and subsequent influence on surface $PM_{2.5}$ and ozone air quality in China due to COVID-19.

Using TROPOMI NO_2 columns in combination with the GEOS-Chem chemical transport model, we estimate weekly NO_x emissions from China in 2019 and 2020 quarter one. The 44.7% decrease of NO_x emission intensity in China from P1 to P2 is substantially higher than the 'holiday effect' in 2019. The nation-wide 53.4% low NO_x emission from China in 2020 lockdown period (P2 and P3) compared to the same period in 2019 indicates a much stronger effect from COVID-19 than previously implemented localized NO_x emission regulation. For the second 4-week period after the Chinese New Year Holiday (P4), NO_x emission intensity started to rebound as the resumption of energy use and economic activity. Interestingly, as of Mar 29, in the last two weeks of 2020 quarter one, NO_x emission has surpassed that in 2019 by 3.9%, indicating a full rebound of NO_x emission from China. Compared to the national total level, NO_x emission from EC region received a much greater impact from COVID-19. NO_x emission in EC during lockdown was 58.4% lower than 2019, and in P4 it was still 22.9% lower than 2019 P4.

Overall, NO_x emission from China in 2020 first quarter is 28.1% lower than that in the same period in 2019, for EC, the ratio is 40.5%. Such large magnitude of decrease in NO_x emission has large influence on surface $PM_{2.5}$ and O_3 air quality. We find from model work that 40.5% decrease of NO_x emission in EC results in 36.5% increase and 12.5% decrease of surface O_3 and $PM_{2.5}$ concentration, respectively. Elevated O_3 and relevant oxidants enhance the secondary aerosol formation through heterogeneous pathway. The complicated interaction between $PM_{2.5}$ and O_3 should be considered in the emission control strategy making process in the future.

CRediT authorship contribution statement

Qianqian Zhang: Methodology, Funding acquisition, Formal analysis, Writing - original draft. **Yuepeng Pan:** Conceptualization, Investigation, Writing - review & editing. **Yuexin He:** Software. **Wendell W. Walters:** Writing - review & editing. **Qianyin Ni:** Resources. **Xuyan Liu:** Investigation. **Guangyi Xu:** Investigation. **Jiali Shao:** Investigation. **Chunlai Jiang:** Investigation.

Declaration of competing interest

The authors declare that they have no known competing financial interests or personal relationships that could have appeared to influence the work reported in this paper.

Acknowledgement

This work is funded by the National Natural Science Foundation of China (No.: 41805098) and the National Key Research and Development Program of China (Grants: 2017YFC0210103). We acknowledge the free use of tropospheric NO_2 column data from the TROPOMI sensor from www.temis.nl.

Appendix A. Supplementary data

Supplementary data to this article can be found online at https://doi.org/10.1016/j.scitotenv.2020.142238.

References

Bauwens, M., Compernolle, S., Stavrakou, T., Müller, J.F., Gent, J., Eskes, H., Levelt, P.F., A R, Veefkind, J.P., Vlietinck, J., Yu, H., Zehner, C., 2020. Impact of coronavirus outbreak on NO_2 pollution assessed using TROPOMI and OMI observations. Geophys. Res. Lett. 47. https://doi.org/10.1029/2020GL087978 (e2020GL087978).

Boersma, K.F., Eskes, H.J., Dirksen, R.J., van der, A.R.J., Veefkind, J.P., Stammes, P., Huijnen, V., Kleipool, Q.L., Sneep, M., Claas, J., Leitão, J., Richter, A., Zhou, Y., Brunner, D., 2011. An improved tropospheric NO_2 column retrieval algorithm for the ozone monitoring instrument. Atmos. Meas. Tech. 4, 1905–1928. https://doi.org/10.5194/amt-4-1905-2011.

Boersma, K.F., Vinken, G.C.M., Eskes, H.J., 2016. Representativeness errors in comparing chemistry transport and chemistry climate models with satellite UV–Vis tropospheric column retrievals. Geosci. Model Dev. 9, 875–898. https://doi.org/10.5194/gmd-9-875-2016.

Ding, J., van der, A.R.J., Eskes, H., Mijling, B., Stavrakou, T., van Geffen, J., Veefkind, P., 2020. Chinese NO_x emission reductions and rebound as a result of the COVID-19 crisis quantified through inversion of TROPOMI NO_2 observations. Geophys. Res. Lett. https://doi.org/10.1002/essoar.10503145.1 accepted.

Field, R.D., Hickman, J.E., Geogdzhayev, I.V., Tsigaridis, K., Bauer, S.E., 2020. Changes in satellite retrievals of atmospheric composition over eastern China during the 2020 COVID-19 lockdowns. Atmos Chem Phys. Discuss. https://doi.org/10.5194/acp-2020-567 (review).

Huang, X., Ding, A., Gao, J., Zheng, B., Zhou, D., Qi, X., Tang, R., Ren, C., Nie, W., Chi, X., Wang, J., Xu, Z., Chen, L., Li, Y., Che, F., Pang, N., Wang, H., Tong, D., Qin, W., Cheng, W., Liu, W., Fu, Q., Chai, F., Davis, S.-J., Zhang, Q., He, K., 2020. Enhanced secondary pollution offset reduction of primary emissions during COVID-19 lockdown in China. National Sciece Review https://doi.org/10.1093/nsr/nwaa137.

Hudman, R.C., Moore, N.E., Mebust, A.K., Martin, R.V., Russell, A.R., Valin, L.C., Cohen, R.C., 2012. Steps towards a mechanistic model of global soil nitric oxide emissions: implementation and space based-constraints. Atmos. Chem. Phys. 12, 7779–7795. https://doi.org/10.5194/acp-12-7779-2012.

Kharol, S.K., Martin, R.V., Philip, S., Boys, B., Lamsal, L.N., Jerrett, M., Brauer, M., Crouse, D.L., McLinden, C., Burnett, R.T., 2015. Assessment of the magnitude and recent trends in satellite-derived ground-level nitrogen dioxide over North America. Atmos. Environ. 118, 236–245. https://doi.org/10.1016/j.atmosenv.2015.08.011.

Lamsal, L.N., Martin, R.V., van Donkelaar, A., Celarier, E.A., Bucsela, E.J., Boersma, K.F., Dirksen, R., Luo, C., Wang, Y., 2010. Indirect validation of tropospheric nitrogen dioxide retrieved from the OMI satellite instrument: insight into the seasonal variation of nitrogen oxides at northern midlatitudes. J. Geophys. Res. 115. https://doi.org/10.1029/2009JD013351.

Lamsal, L.N., Martin, R.V., Padmanabhan, A., van Donkelaar, A., Zhang, Q., Sioris, C.E., Chance, K., Kurosu, T.P., Newchurch, M.J., 2011. Application of satellite observations for timely updates to global anthropogenic NO_x emission inventories. Geophys. Res. Lett. 38, L05810. https://doi.org/10.1029/2010GL046476.

Le, T., Wang, Y., Liu, L., Yang, J., Yung, Y., Li, G., Seinfeld, J.-H., 2020. Unexpected air pollution with marked emission reductions during the COVID-19 outbreak in China. Science 369, 5. https://doi.org/10.1126/science.abb7431.

Li, M., Zhang, Q., Kurokawa, J.-i., Woo, J.-H., He, K., Lu, Z., Ohara, T., Song, Y., Streets, D.G., Carmichael, G.R., Cheng, Y., Hong, C., Huo, H., Jiang, X., Kang, S., Liu, F., Su, H., Zheng, B., 2017. MIX: a mosaic Asian anthropogenic emission inventory under the international collaboration framework of the MICS-Asia and HTAP. Atmos. Chem. Phys. 17, 935–963. https://doi.org/10.5194/acp-17-935-2017.

Liu, F., Page, A., Strode, S.A., Yoshida, Y., Choi, S., Zheng, B., Lamsal, L.N., Li, C., Krotkov, N.A., Eskes, H., van der, A.R., Veefkind, P., Levelt, P.F., Hauser, O.P., Joiner, J., 2020. Abrupt decline in tropospheric nitrogen dioxide over China after the outbreak of COVID-19. Sci. Adv. 6, eabc2992. https://doi.org/10.1126/sciadv.abc2992.

Lorente, A., Boersma, K.F., Eskes, H.J., Veefkind, J.P., van Geffen, J., de Zeeuw, M.B., Denier van der Gon, H.A.C., Beirle, S., Krol, M.C., 2019. Quantification of nitrogen oxides emissions from build-up of pollution over Paris with TROPOMI. Sci. Rep. 9, 20033. https://doi.org/10.1038/s41598-019-56428-5.

Martin, R.V., 2003. Global inventory of nitrogen oxide emissions constrained by space-based observations of NO_2 columns. J. Geophys. Res. 108. https://doi.org/10.1029/2003JD003453.

Murray, L., Jacob, D., Logan, J.A., Hudman, R.C., Koshak, W., 2012. Optimized regional and interannual variability of lightning in a global chemical transport model constrained by LIS/OTD satellite data. J. Geophys. Res.: Atmospheres, 117 https://doi.org/10.1029/2012JD017934.

Myllyvirta, L., 2020. Coronavirus temporarily reduced China's CO_2 emission by a quarter. Carbonbrief https://www.carbonbrief.org/analysis-coronavirus-has-temporarily-reduced-chinas-co2-emissions-by-a-quarter.

Shah, V., Jacob, D.J., Li, K., Silvern, R.F., Zhai, S., Liu, M., Lin, J., Zhang, Q., 2020. Effect of changing NO_x lifetime on the seasonality and long-term trends of satellite-observed tropospheric NO_2 columns over China. Atmos. Chem. Phys. 20, 1483–1495. https://doi.org/10.5194/acp-20-1483-2020.

Shi, X., Brasseur, G.P., 2020. The response in air quality to the reduction of Chinese economic activities during the COVID-19 outbreak. Geophys. Res. Lett. 47. https://doi.org/10.1029/2020GL088070.

Sun, Y., Lei, L., Zhou, W., Chen, C., He, Y., Sun, J., Li, Z., Xu, W., Wang, Q., Ji, D., Fu, P., Wang, Z., Worsnop, D.R., 2020. A chemical cocktail during the COVID-19 outbreak in Beijing, China: insights from six-year aerosol particle composition measurements during the Chinese New Year holiday. Sci. Total Environ. 742, 140739. https://doi.org/10.1016/j.scitotenv.2020.140739.

Tan, P.-H., Chou, C., Liang, J.-Y., Chou, C.C.K., Shiu, C.-J., 2009. Air pollution "holiday effect" resulting from the Chinese New Year. Atmos. Environ. 43, 2114–2124. https://doi.org/10.1016/j.atmosenv.2009.01.037.

Tan, Z., Rohrer, F., Lu, K., Ma, X., Bohn, B., Broch, S., Dong, H., Fuchs, H., Gkatzelis, G.I., Hofzumahaus, A., Holland, F., Li, X., Liu, Y., Liu, Y., Novelli, A., Shao, M., Wang, H., Wu, Y., Zeng, L., Hu, M., Kiendler-Scharr, A., Wahner, A., Zhang, Y., 2018. Wintertime photochemistry in Beijing: observations of RO_x radical concentrations in the North China Plain during the BEST-ONE campaign. Atmos. Chem. Phys. 18, 12391–12411. https://doi.org/10.5194/acp-18-12391-2018.

van Geffen, J., Boersma, K.F., Eskes, H., Sneep, M., ter Linden, M., Zara, M., Veefkind, J.P., 2020. S5P TROPOMI NO_2 slant column retrieval: method, stability, uncertainties and comparisons with OMI. Atmos. Meas. Tech. 13, 1315–1335. https://doi.org/10.5194/amt-13-1315-2020.

Vinken, G.C.M., Boersma, K.F., van Donkelaar, A., Zhang, L., 2014. Constraints on ship NO_x emissions in Europe using GEOS-Chem and OMI satellite NO_2 observations. Atmos. Chem. Phys. 14, 1353–1369. https://doi.org/10.5194/acp-14-1353-2014.

Visser, A.J., Boersma, K.F., Ganzeveld, L.N., Krol, M.C., 2019. European NO_x emissions in WRF-Chem derived from OMI: impacts on summertime surface ozone. Atmos. Chem. Phys. 19, 11821–11841. https://doi.org/10.5194/acp-19-11821-2019.

Wang, S., Zhao, M., Xing, J., Wu, Y., Zhou, Y., Lei, Y., He, K., Fu, L., Hao, J.M., 2010. Quantifying the air pollutants emission reduction during the 2008 Olympic games in Beijing. Environ. Sci. Technol. 44 (7). https://doi.org/10.1021/es9028167.

Wang, Y.X., Zhang, Q.Q., He, K., Zhang, Q., Chai, L., 2013. Sulfate-nitrate-ammonium aerosols over China: response to 2000–2015 emission changes of sulfur dioxide, nitrogen oxides, and ammonia. Atmos. Chem. Phys. 13, 2635–2652. https://doi.org/10.5194/acp-13-2635-2013.

Xu, G., Zhang, Q., Yao, Y., Zhang, X., 2020. Changes in $PM_{2.5}$ sensitivity to NO_x and NH_3 emissions due to a large decrease in SO_2 emissions from 2013 to 2018. Atmospheric and Oceanic Science Letters 13, 6. https://doi.org/10.1080/16742834.2020.1738009.

Zhang, Q., Wang, Y., Ma, Q., Yao, Y., Xie, Y., He, K., 2015. Regional differences in Chinese SO_2 emission control efficiency and policy implications. Atmos. Chem. Phys. 15, 6521–6533. https://doi.org/10.5194/acp-15-6521-2015.

Zhang, L., Shao, J., Lu, X., Zhao, Y., Hu, Y., Henze, D.K., Liao, H., Gong, S., Zhang, Q., 2016. Sources and processes affecting fine particulate matter pollution over North China: an adjoint analysis of the Beijing APEC period. Environ. Sci. Technol. 50, 8731–8740. https://doi.org/10.1021/acs.est.6b03010.

Zhang, Q., Ma, Q., Zhao, B., Liu, X., Wang, Y., Jia, B., Zhang, X., 2018. Winter haze over North China Plain from 2009 to 2016: influence of emission and meteorology. Environ. Pollut. 242, 1308–1318. https://doi.org/10.1016/j.envpol.2018.08.019.

Zhang, Q., Pan, Y., He, Y., Zhao, Y., Zhu, L., Zhang, X., Xu, X., Ji, D., Gao, J., Tian, S., Gao, W., Wang, Y., 2019. Bias in ammonia emission inventory and implications on emission control of nitrogen oxides over North China Plain. Atmos. Environ. 214. https://doi.org/10.1016/j.atmosenv.2019.116869.

Zhang, R., Zhang, Y., Lin, H., Feng, X., Fu, T.-M., Wang, Y., 2020. NO_x emission reduction and recovery during COVID-19 in East China. Atmosphere 11, 433. https://doi.org/10.3390/atmos11040433.

Zhao, B., Wang, S.X., Liu, H., Xu, J.Y., Fu, K., Klimont, Z., Hao, J.M., He, K.B., Cofala, J., Amann, M., 2013. NO_x emissions in China: historical trends and future perspectives. Atmos. Chem. Phys. 13, 9869–9897. https://doi.org/10.5194/acp-13-9869-2013.